An Integrated Tunable Electrical-Balance Filter with >60dB Stopband Attenuation and 1.75-3.7GHz Stopband Tuning Range

Barend van Liempd [*+], Benjamin Hershberg [*], Piet Wambacq [*+], Jan Craninckx [*]
[*] Imec, Leuven, Belgium
[+] Vrije Universiteit Brussel, Dept. of Electronics and Informatics, Brussels, Belgium

***Abstract*— This paper proposes the concept of electrical balance filters to enable integrated, tunable RF filters, where a pass- and stopband are designed by the change in electrical-balance across frequency. These filters can be constructed using low Q integrated LC resonators. The stopband frequency is the frequency where two on chip balance networks are tuned to be equal in impedance or 'balanced', while the passband frequency is the frequency where the balance condition is disturbed as much as possible for low insertion loss. A 1.5mm2 electrical balance low-pass filter prototype is implemented in 0.18µm SOI CMOS. It has <4dB insertion loss at 1GHz with a >60dB, >33MHz stopband tunable from 1.75 to 3.7 GHz.**

Keywords*— Electrical-balance, RF, filter, tunable filter, impedance-based filtering, low-loss, high attenuation.

I. INTRODUCTION

With the advance of the *Internet of Things*, wireless devices must support an ever-increasing amount of bands and allow multi-standard co-existence. Due to the proliferation of carrier aggregation (CA), transmit-to-receive (TX/RX) isolation within the device is critical. Integration of the more bulky parts of a wireless system, namely the front-end module (FEM), is a key driver that allows to implement RF capabilities in ever more *things*.

For example, the harmonic distortion product of a TX operating below 1GHz can end up directly in-band for an RX operating within the ISM band. For CA, even off-chip fixed-frequency multiplexer filters based on bulk- or surface acoustic wave (BAW/SAW) resonators have difficulties to achieve the required amount of attenuation.

Various approaches and technologies have been considered to enable tunable RF filters [1]-[3]. High Q-factor resonators provide filtering structures with desirable passband and stopband characteristics. However, integrating such tunable filters alongside other transceiver circuits in CMOS is limited by the large dimensions of resonators and transmission lines.

Recently, electrical-balance (EB) duplexers have been introduced as a means to replace fixed-frequency duplexers for frequency-division duplex (FDD) and provide frequency-flexible TX-to-RX isolation [3],[5]. Also, EB duplexers are able to address the unique requirements of in-band full-duplex (IBFD) radios since they provide isolation when the TX and RX operate at the same time and frequency, much like a high-isolation circulator. Fig. 1 shows an example tunable FEM architecture enabled by tunable RF filters, that would allow for TDD/FDD/IBFD multi-standard co-existence, antenna sharing for various bands and CA.

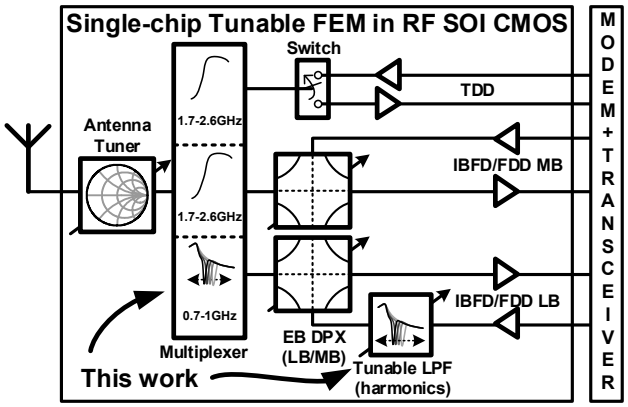

Fig. 1. Tunable RF filters in an example many-band, multi-standard antenna interface.

This paper proposes, for the first time, the use of the electrical-balance concept for the implementation of integrated, tunable, RF *filters* that achieve high attenuation using only low-Q (Q_{peak}<20) passives. The concept is that electrical imbalance in an EB duplexer can reduce the isolation to such a poor level, that it could be considered as *passband insertion loss* rather than isolation. Simultaneously, isolation (i.e. electrical-balance) is maintained at a second (stopband) frequency and hence is considered *stopband attenuation*. To construct such a filter, a second tunable on-chip balance network is added. The (im)balance is then controlled without the need for adaptive tuning, as in the EB-duplexer case.

A tunable EB-based LPF design is presented to demonstrate the concept of these promising integrated filters. The 1.5mm2 prototype is implemented in 0.18µm SOI CMOS. It uses stacked switches for power handling, and coupling capacitors implement the hybrid junction to minimize loss and area. Compared to recent MEMS-based tunable filters, this work has 2 orders of magnitude better stopband attenuation and tuning range, but 2 orders of magnitude less required area.

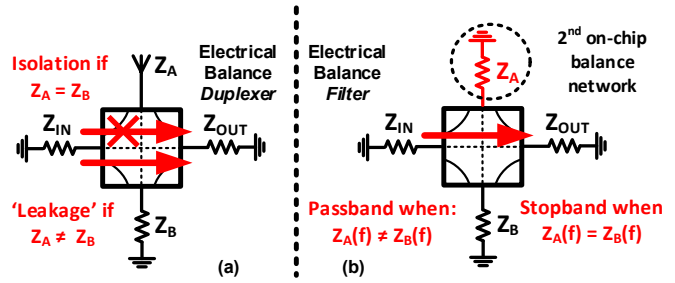

Fig. 2. (a) EB duplexer based on a hybrid junction: electrical balance (Z_A=Z_B) causes TX signal cancellation at the RX port; (b) EB filter using a second on-chip balance network: electrical *im*balance ($Z_A \neq Z_B$) creates a low-loss passband while maintaining cancellation at a second frequency.

II. EB Filter Operating Principle

The EB filter is a special, hitherto unrecognized use-case of a hybrid junction [6]. Hybrid junctions were first used in telephony networks for port-to-port isolation at KHz-frequencies, and relatively recently re-introduced to operate at RF for the integration of EB *duplexers* [3],[5]. More recently, hybrid junctions have also been used to implement tunable RF *phase shifters* [7].

Fig. 2(a) shows a hybrid junction implementing an EB duplexer to provide cancellation of the TX signal at the RX node at any frequency where Z_A=Z_B, with Z_A the antenna impedance and Z_B the balance network impedance. Cancellation occurs because a hybrid junction provides signal subtraction in the signal path, causing a notch in the transfer function where the two impedances are equal. Electrical-imbalance in a hybrid junction, written as $Z_A \neq Z_B$, can reduce the TX-to-RX isolation to very poor levels. It can be shown that an ideal hybrid junction would have 0dB 'isolation' and hence a perfect passband in the extreme case where Z_A='short' and Z_B='open'. This property is exploited to enable a filter structure with a passband.

In the EB filter in Fig. 2(b), the antenna is omitted and a hybrid junction is used with two (on-chip) impedances Z_A and Z_B, such that Z_A=Z_B at one frequency (stopband) and $Z_A \neq Z_B$ at another frequency (passband). Unlike the duplexer case, where Z_A varies with the antenna environment, the filter Z_A and Z_B do not vary across time and the stopband frequency is thus much simpler to control.

Fig. 3 shows two balance networks that exhibit favorable characteristics for implementation of EB filters. The first network (Z_A) is a parallel L-C resonator and the second network (Z_B) is a series L-C resonator. Z_A is a short for low frequencies and inductive (+j) up to its resonance frequency $f_{res,A}$, and capacitive (-j) for frequencies beyond. Inversely, Z_B is an open for low frequencies and then first capacitive (-j) before resonance $f_{res,B}$, after which it becomes inductive (+j) for frequencies >$f_{res,B}$. By choosing $f_{res,A} < f_{res,B}$, a low-pass, high-stop filter is achieved (Fig. 4). In this way, a desirable phase inversion is obtained while EB-based cancellation is enabled at the stopband.

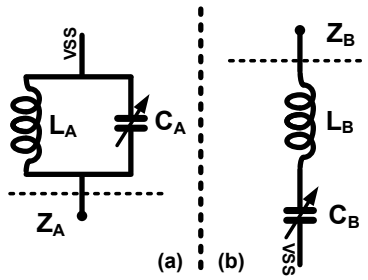

Fig. 3. Proposed tunable balance networks: (a) Z_A & (b) Z_B.

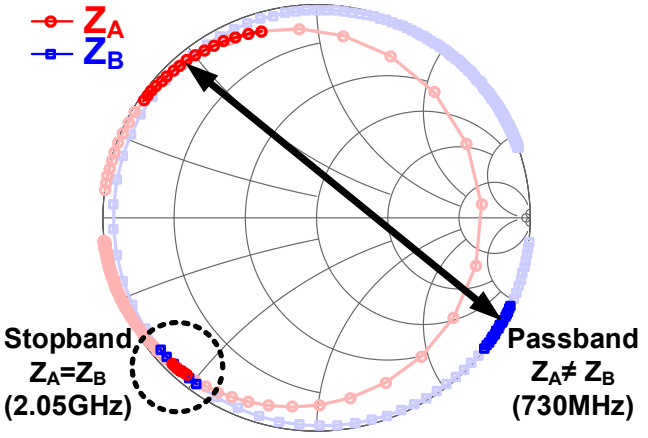

Fig. 4. Simulated Z_A and Z_B in a 50Ω-Smith chart for an LPF design: passband at 0.73GHz and stopband at 2.05GHz.

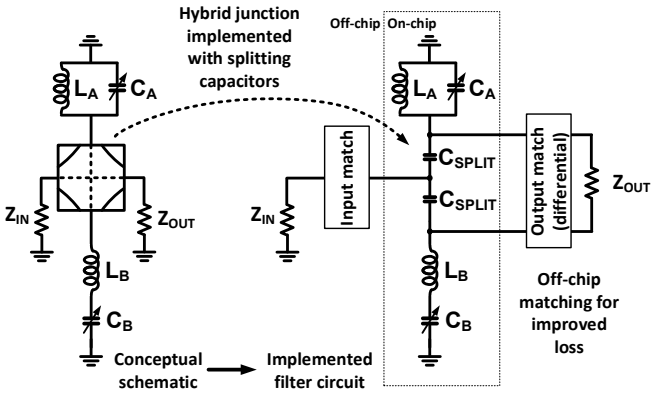

Fig. 5. EB filter conceptual and implemented schematic.

III. Example EB Filter Implementation

Fig. 5 shows the schematic of an LPF EB filter implemented as a demonstrator of the concept explained in the previous section. It is based on the proposed impedances Z_A and Z_B. Unlike EB duplexers, where a hybrid transformer is often used to implement the hybrid junction [6], this work achieves signal subtraction using coupling capacitors, like [7]. Therefore, the filter has a common mode and a differential mode port. Note that this structure does have the drawback of

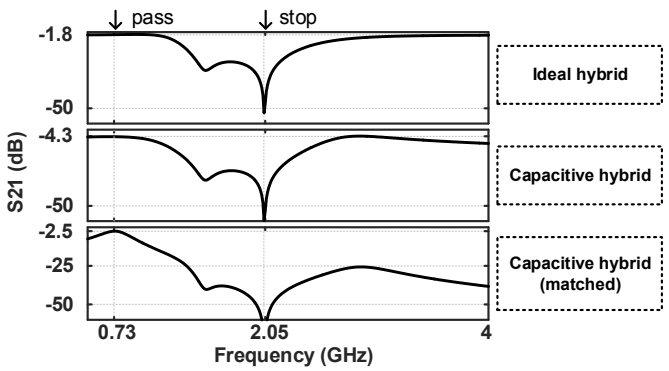

Fig. 6. Simulated S21 for the EB filter with an ideal hybrid, a capacitive hybrid and an input/output matched capacitive hybrid.

requiring a single-to-differential converter between the filter and other circuits, but conceptually a hybrid transformer can be used to obtain a fully single-ended operation when common-mode to differential-mode performance is critical, at the cost of chip area [5].

The simulated difference in performance between using an ideal hybrid transformer, splitting capacitors or splitting capacitors with input/output matching is shown in Fig. 6. After matching, loss is improved. Fig. 7 shows that the cancellation frequency is tuned for different combinations of C_A and C_B. The passband frequency could be tuned independently of the stopband by tuning C_{SPLIT}, since it does not impact the electrical balance $|Z_A-Z_B|$. The prototype uses a fixed 2.5pF MIM capacitor for C_{SPLIT}.

L_A is a 2.6nH inductor and L_B is a 5.12nH inductor. Both L_A and L_B use 2 stacked RF metals to achieve Q>18. C_A/C_B are 6-bit 1.17-6.5pF and 5-bit 0.2-1.65pF tunable capacitor banks, respectively. They are implemented using a similar circuit topology as in [5], using two stacked SOI switches for moderate power handling capability. Capacitors in both Z_A and Z_B can be tuned to achieve sufficiently high accuracy EB for high stopband attenuation, as shown in Fig. 7. Indeed, for 50dB of attenuation, 50dB balancing accuracy is required, just like in EB duplexers [5].

IV. Measurement Results

Fig. 8 shows a micrograph of the 1.5mm^2 EB filter prototypes fabricated in a 0.18µm RF SOI CMOS process. The chips were bonded onto an FR4 test board. To avoid the need for an external (imperfectly balanced) balun, the filter is tested using a 4-port R&S ZVA24 network analyzer, such that common-mode and a differential-mode testing ports are directly available. Instead of adding physical off-chip matching components, the ZVA24 option called 'virtual embedding' was used to optimize insertion loss, using Q=25 inductor (1x) and capacitor (3x) components.

The common-to-differential S21 is shown in Fig. 9 for various tuning settings, illustrating that the stopband can be tuned from 1.73GHz to 3.7GHz, with a stopband bandwidth of

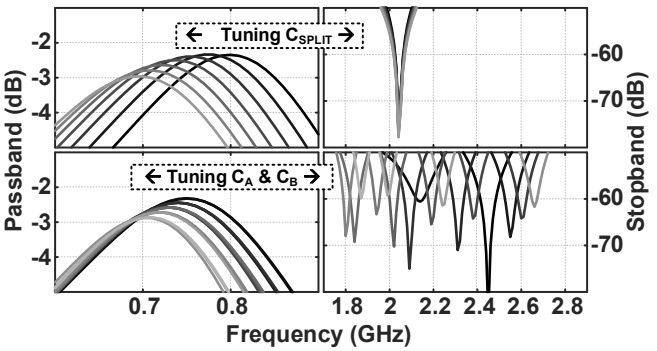

Fig. 7. Simulated passband and stopband for ±30% tuned C_{SPLIT} (top) and C_A & C_B (bottom) showing independent tuning.

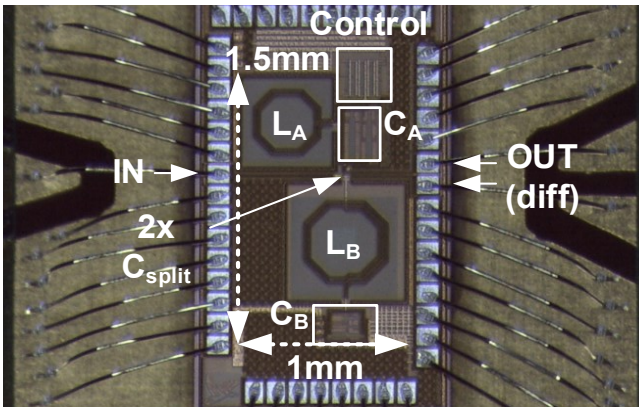

Fig. 8. Chip photograph of the 1.5mm^2 electrical-balance filter prototype in 0.18µm SOI CMOS, bonded to an FR4 test board.

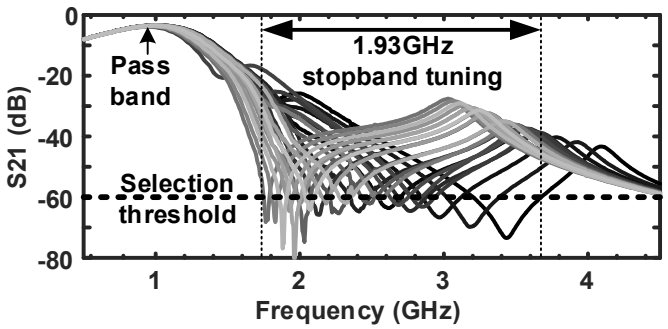

Fig. 9. Measured S21 for 24 out of 1024 C_A & C_B combinations with >60dB attenuation and >33MHz stopband BW (using 'virtual embedding' for matching purposes).

at least 33MHz. A total of 1024 combinations were tested (C_AxC_B=32x32). Not all combinations produce a cancellation notch. Fig. 9 shows a subset of 24 curves to summarize the performance. The subset of the data was selected for >60dB attenuation across >33MHz BW. The S21 characteristics match simulation very well, with a higher passband frequency since a smaller C_{SPLIT} was used (Fig. 6 and Fig. 7 use a 5pF capacitor). From Fig. 9, the low-pass matching improves stopband attenuation at higher frequencies as intended.

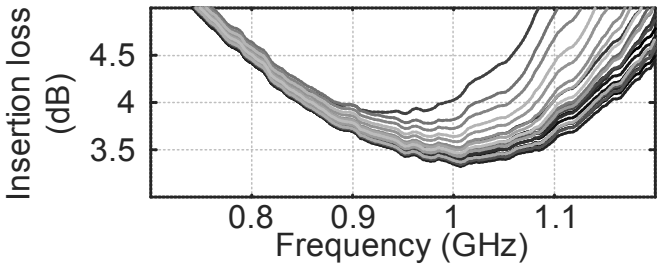

Fig. 10. Measured passband insertion loss (from Fig. 9 data).

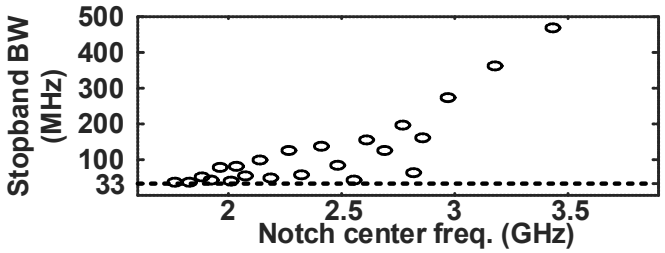

Fig. 11. Measured stopband notch bandwidth versus center frequency (extracted from Fig. 9 data) for a 33MHz threshold.

Fig. 10 shows 3.4-4.5dB measured insertion loss for 0.82-1.05GHz. As per simulation (Fig. 7), C_{SPLIT} could be made tunable to allow for tuning and compensation of the frequency shift that occurs when C_A and C_B are tuned. Compared to simulation (Fig. 7), the measured loss is about 1dB worse due to mismatch, matching component Q, and the Q of C_{SPLIT}. Not shown is S11, which is <-10dB across the entire passband.

Fig. 11 shows the measured stopband notch bandwidth versus the notch center frequency, extracted for the same settings. For >60dB of stopband attenuation, at least 33MHz of notch bandwidth is achieved.

Table 1 compares this work to two tunable RF filters based on high-Q resonators that use RF MEMS switches for pass/stopband tuning. In summary, this work achieves >300x size reduction through CMOS integration and larger stop-band tuning range at >20dB higher stopband attenuation, while having 1 to 3dB worse insertion loss.

V. Conclusions

This paper proposes, for the first time, the concept of electrical-balance filters for integrating tunable RF filters, critical to further develop a frequency-flexible, tunable FEM for future wireless applications. This filter avoids bulky transmission lines and high-Q resonators altogether.

A low-pass prototype filter is implemented in 0.18µm RF SOI CMOS and achieves very promising results. The 1.5mm^2 LPF has a tunable stopband from 1.75-3.7GHz, i.e. 1.95GHz aggregated tunable bandwidth, with <4dB insertion loss at 1GHz. A stopband attenuation of >60dB with >33MHz stopband bandwidth is measured. Future work could address the moderate-high insertion loss, and Z_A/Z_B topologies that enable a BPF or HPF.

TABLE I. Comparison with Tunable RF Filters.

	This work	**[1]**	**[2]**
Technology	0.18µm SOI CMOS	RF MEMS	RF MEMS
Area [mm^2]	1.5	>2275 **	>500 **
Filter type	Low-pass	Band-pass	Band-stop
Passband [GHz]	0.82-1.05	1.2-1.6	<2.5GHz ****
Insertion loss [dB]	3.4-4.5	1-3.5	<0.8
1dB-BW [MHz]	>250	>75	DC-to-Stop
Tunable?	No *	Yes	No
Tuning range [MHz]	N/A	400	N/A
Stopband [GHz]	1.75-3.7	<2.2 ***	1.13-2.67
Attenuation [dB]	>60	>35	>40
BW [MHz]	>33 (33-480)	Pass-to-2.2	115±25
Tunable?	Yes	No	Yes
Tuning range [MHz]	1950 (60dB)	N/A	1540 (40dB)

* Can be implemented with tunable C_{SPLIT}.
** Estimated from PCB photo.
*** Here, frequencies higher than the passband, up to a spurious response of the filter at 2.2GHz, were considered as the stopband.
**** When the stopband is tuned, passband is anywhere between DC to where the stopband starts.

Acknowledgment

The authors thank S. Ariumi (muRata) for valuable discussions and acknowledge J. Borremans (imec) for the idea of using coupling capacitors instead of a transformer.

References

[1] V. Sekar, K. Entesari, "A Half-Mode Substrate-Integrated-Waveguide Tunable Filter Using Packaged RF MEMS Switches," *IEEE Microw. and Wirel. Comp. Letters*, Vol.22, No.7, pp.336-338, July 2012.

[2] C.-C. Cheng, G.M. Rebeiz, "A Three-Pole 1.2–2.6-GHz RF MEMS Tunable Notch Filter With 40-dB Rejection and Bandwidth Control," *IEEE Trans. Microw. Theory Techn.*, Vol.60, No.8, pp.2431-2438, Aug. 2012.

[3] T. Ogami et al., "A new tunable filter using love wave resonators for reconfigurable RF," *IEEE MTT-S Int.Microw. Symp. Dig.*, 1-6 June 2014

[4] M. Mikhemar, H. Darabi, A. Abidi, "A tunable integrated duplexer with 50dB isolation in 40nm CMOS," *IEEE Int. Solid-State Circuits Conf. (ISSCC) Dig. Tech. Papers*, pp.386-387, 8-12 Feb. 2009

[5] B. van Liempd et al., "A +70dBm IIP3 Single-Ended Electrical-Balance Duplexer in 0.18µm SOI CMOS," *IEEE ISSCC Dig. Tech. Papers*, pp.32-33, 22-26 Feb. 2015.

[6] E. Sartori, "Hybrid Transformers," *IEEE Trans. Parts, Materials and Packaging*, Vol.4, No.3, pp.59-66, Sep 1968.

[7] B. van Liempd, P. Wambacq, J. Craninckx, "An Inductorless Electrical-Balance 360° Phase Shifter for 0.5-1.15GHz in 0.18µm CMOS," *IEEE European Microwave Integrated Circuits Conference*, pp.132-135, 7-8 Sept. 2015.